https://doi.org/10.5755/j02.eie.40870 ELEKTRONIKA IR ELEKTROTECHNIKA, ISSN 1392-1215, VOL. 31, NO. 3, 2025

An Exact Analysis of Fine Resolution Frequency Estimation Method from Three DFT Samples: Windowed Data Case

Betofe Mboyo Keyta, Erdogan Dilaveroglu*
Department of Electrical and Electronics Engineering, Bursa Uludag University, 16059 Bursa, Turkiye
*511905001@ogr.uludag.edu.tr; *dilaver@uludag.edu.tr*

***Abstract*—Frequency estimation for a single complex sinusoid in noise is a fundamental problem in signal processing. A suboptimal but simple frequency estimator, known as Jacobsen estimator, which is based on three discrete Fourier transform (DFT) samples, gives good bias performance without the need to increase the DFT size. Candan has modified the Jacobsen estimator by adding a so-called bias correction factor to further reduce the bias of the estimator. In addition to bias considerations, a number of asymptotic variance expressions of the estimators were performed in the literature. However, these expressions are valid only for signal frequencies located very near a DFT bin index. In this paper, with the use of a simple variance analysis technique, an accurate general variance expression for arbitrary frequency locations is derived for the case of windowed data. A general method for calculating the bias correction factor is also proposed. The variance expression is examined for the cosine-sum window family. An approximate variance formula for sufficiently large data record lengths is also given for windows from this family. Computer simulations are included to validate the theoretical results.**

***Index Terms*—Additive white noise; Analysis of variance; Discrete Fourier Transform; Frequency estimation.**

I. INTRODUCTION

The problem of sinusoidal frequency estimation has been frequently studied in the signal processing literature due to its wide range of applications. Consider the following data model consisting of a complex sinusoid in noise

$$x_n = \alpha e^{j\phi} \exp\left(j2\pi fn/N\right) + e_n,\ n = 0,1,\ldots,N-1, \qquad (1)$$

where α , ϕ, and f are real-valued unknown deterministic parameters, which are amplitude, phase, and frequency of the complex sinusoid, e_n is assumed to be a zero-mean complex white noise process with unknown variance σ^2. The frequency is decomposed into an integer bin index k_0 and a fractional term δ as $f = k_0 + \delta$ with $|\delta| \le 0.5$.

The approach to estimate f from the N samples of x_n proposed by Jacobsen [1] and later modified by Candan [2] uses the three (the peak and its two neighbours) discrete Fourier transform (DFT) samples $\{X_k\}_{k=0}^{N-1}$ of the windowed data $\{w_n x_n\}_{n=0}^{N-1}$. Here w_n is a real-valued window function that is used to mitigate spectral leakage from interferences [3]. Let k_0 be the peak index. Assuming that the peak is correctly detected, i.e., the parameter k_0 is known, the fractional part δ of the frequency is estimated via

$$\hat{\delta} = c_N \operatorname{Re}\left(\frac{X_{k_0-1} - X_{k_0+1}}{2X_{k_0} - X_{k_0-1} - X_{k_0+1}}\right), \qquad (2)$$

where c_N is the bias correction factor added in [2] to reduce the bias of the estimator in [1]; for a specific window function, c_N depends only on N.

For small values of δ, an expression for the variance of the estimator $\hat{\delta}$ has been derived in [4] for the rectangle window case ([4], (11)), and a mean square error expression for $\hat{\delta}$ is given in [5] for the case of arbitrary windows ([5], (13)). However, these expressions, which are developed under small δ assumption, give inaccurate results when $|\delta|$ is relatively large.

Recently, we have derived an exact closed-form expression for the variance of $\hat{\delta}$ for the rectangle window case [6]. In this paper, we extend our work to any windows applied to the data, including the rectangle window. With the use of a Taylor series expansion technique (see, e.g., [7]), an exact general variance expression for $\hat{\delta}$ is derived in Section II. A general method for the computation of the bias correction factor c_N is also given. The variance expression is examined for the case of cosine-sum windows in Section III. For this family of windows, an approximate variance expression for sufficiently large N is also included. Computer simulations are presented in Section IV to validate the theoretical results. Finally, conclusions are drawn in Section V.

II. EXACT VARIANCE DERIVATION

Let

Manuscript received 19 March, 2025; accepted 6 June, 2025.

$$\hat{d}(\boldsymbol{\theta}) = \mathrm{Re}\left(\frac{X_{k_0-1} - X_{k_0+1}}{2X_{k_0} - X_{k_0-1} - X_{k_0+1}} \right) \tag{3}$$

with

$$\boldsymbol{\theta} = \left[\bar{X}_{k_0-1}, \tilde{X}_{k_0-1}, \bar{X}_{k_0}, \tilde{X}_{k_0}, \bar{X}_{k_0+1}, \tilde{X}_{k_0+1} \right]^{\mathrm{T}}, \tag{4}$$

where the superscript T denotes the transpose. For notational convenience, here and onwards, an over bar denotes the real part of the quantity beneath it, and an over tilde denotes the imaginary part, i.e., $\bar{X} = \mathrm{Re}\{X\}$ and $\tilde{X} = \mathrm{Im}\{X\}$ for a complex quantity X.

Let $\boldsymbol{\theta}_0 = E\{\boldsymbol{\theta}\}$, i.e., the mean of $\boldsymbol{\theta}$. It is calculated as (see Appendix A)

$$\boldsymbol{\theta}_0 = \left[\bar{g}(\delta+1), \tilde{g}(\delta+1), \bar{g}(\delta), \tilde{g}(\delta), \bar{g}(\delta-1), \tilde{g}(\delta-1) \right]^{\mathrm{T}}, \tag{5}$$

where

$$g(\delta+l) = \alpha e^{j\phi} \sum_{n=0}^{N-1} w_n \exp\left(j\frac{2\pi}{N}(\delta+l)n \right) \tag{6}$$

for $l = 0, 1$ and -1. For sufficiently large N and/or signal-to-noise ratio (SNR), defined as $\mathrm{SNR} = \alpha^2/\sigma^2$, $\boldsymbol{\theta}$ will be in the vicinity of $\boldsymbol{\theta}_0$, and a first order Taylor expansion of $\hat{d}(\boldsymbol{\theta})$ around $\boldsymbol{\theta}_0$ yields

$$\hat{d}(\boldsymbol{\theta}) \cong \hat{d}(\boldsymbol{\theta}_0) + \mathbf{v}^{\mathrm{T}}(\boldsymbol{\theta} - \boldsymbol{\theta}_0), \tag{7}$$

where $\mathbf{v} = \nabla \hat{d}(\boldsymbol{\theta})\big|_{\boldsymbol{\theta}=\boldsymbol{\theta}_0}$ is the gradient of $\hat{d}(\boldsymbol{\theta})$ evaluated at $\boldsymbol{\theta} = \boldsymbol{\theta}_0$, which is a function of N, α, ϕ, and δ for a particular window. From (7), it follows that

$$E\left\{\hat{d}(\boldsymbol{\theta})\right\} \cong \hat{d}(\boldsymbol{\theta}_0) \tag{8}$$

and

$$\mathrm{var}\left(\hat{d}(\boldsymbol{\theta})\right) \cong \mathbf{v}^{\mathrm{T}}\mathbf{C}_{\boldsymbol{\theta}}\mathbf{v}, \tag{9}$$

where $\mathbf{C}_{\boldsymbol{\theta}} = E\left\{(\boldsymbol{\theta} - \boldsymbol{\theta}_0)(\boldsymbol{\theta} - \boldsymbol{\theta}_0)^{\mathrm{T}}\right\}$ is the covariance matrix of $\boldsymbol{\theta}$. $\mathbf{C}_{\boldsymbol{\theta}}$ is derived as (see Appendix A)

$$\mathbf{C}_{\boldsymbol{\theta}} = \frac{\sigma^2}{2} \begin{bmatrix} \mathbf{Q}_0 & \mathbf{Q}_1 & \mathbf{Q}_2 \\ \mathbf{Q}_1^{\mathrm{T}} & \mathbf{Q}_0 & \mathbf{Q}_1 \\ \mathbf{Q}_2^{\mathrm{T}} & \mathbf{Q}_1^{\mathrm{T}} & \mathbf{Q}_0 \end{bmatrix}, \tag{10}$$

where

$$\mathbf{Q}_k = \begin{bmatrix} \bar{q}_k & \tilde{q}_k \\ -\tilde{q}_k & \bar{q}_k \end{bmatrix} \tag{11}$$

and

$$q_k = \sum_{n=0}^{N-1} w_n^2 \exp\left(-j\frac{2\pi}{N}kn \right) \tag{12}$$

for $k = 0, 1, 2$. Inserting (10) into (9), and noting that $\mathrm{var}\left(\hat{\delta}\right) = c_N^2\, \mathrm{var}\left(\hat{d}\right)$, the variance of $\hat{\delta}$ can be expressed in a nonmatrix form as

$$\begin{aligned} \mathrm{var}\left(\hat{\delta}\right) \cong c_N^2 \sigma^2 \Big(& \frac{q_0}{2}\|\mathbf{v}\|^2 + \bar{q}_1(v_1v_3 + v_2v_4 + v_3v_5 + v_4v_6) + \\ & + \tilde{q}_1(v_1v_4 - v_2v_3 + v_3v_6 - v_4v_5) + \bar{q}_2(v_1v_5 + v_2v_6) + \\ & + \tilde{q}_2(v_1v_6 - v_2v_5) \Big). \end{aligned} \tag{13}$$

For the rectangle window, $q_0 = N$, $q_1 = q_2 = 0$, and (13) becomes $\mathrm{var}\left(\hat{\delta}\right) \cong \frac{1}{2} c_N^2 N \sigma^2 \|\mathbf{v}\|^2$, which is identical to the expression in ([6], (13)).

It is shown in Appendix B that the variance expression in (13) does not depend on ϕ, so we can take $\phi = 0$ for the calculation of $\mathbf{v}$ in (13). Furthermore, since the elements of $\nabla \hat{d}(\boldsymbol{\theta})$ are of the form $\left(\sum \theta_i\theta_j\theta_k\right) / \left(\sum \theta_l\theta_m\right)^2$, α appears in each element of $\mathbf{v}$ as the multiplier α^{-1}. Thus, the expression in (13) can be rewritten in a more compact form as

$$\mathrm{var}\left(\hat{\delta}\right) \cong \frac{c_N^2 \lambda_N(\delta)}{N\,\mathrm{SNR}}, \tag{14}$$

where

$$\begin{aligned} \lambda_N(\delta) = & \frac{q_0}{2}\|\breve{\mathbf{v}}\|^2 + \bar{q}_1(\breve{v}_1\breve{v}_3 + \breve{v}_2\breve{v}_4 + \breve{v}_3\breve{v}_5 + \breve{v}_4\breve{v}_6) + \\ & + \tilde{q}_1(\breve{v}_1\breve{v}_4 - \breve{v}_2\breve{v}_3 + \breve{v}_3\breve{v}_6 - \breve{v}_4\breve{v}_5) + \bar{q}_2(\breve{v}_1\breve{v}_5 + \breve{v}_2\breve{v}_6) + \\ & + \tilde{q}_2(\breve{v}_1\breve{v}_6 - \breve{v}_2\breve{v}_5) \end{aligned} \tag{15}$$

with

$$\breve{\mathbf{v}} = \sqrt{N} \cdot \mathbf{v}\big|_{\alpha=1, \phi=0}, \tag{16}$$

which is the normalised gradient vector $\mathbf{v}$ after substitutions $\alpha = 1$ and $\phi = 0$.

The variance expression in (14) is independent of ϕ, and inversely proportional to SNR and N (in the following sections, it is shown that both c_N and $\lambda_N(\delta)$ in (14) depend very weakly on N).

Note that (14) gives the variance of the Jacobsen estimator in [1] for $c_N = 1$.

A. Calculation of the Bias Correction Factor

For a particular window, the role of the bias correction factor c_N is to reduce the bias of the estimator $\hat{\delta}$. From (8), the mean and bias of $\hat{\delta} = c_N\hat{d}$ are given by

$$E\left\{\hat{\delta}(\boldsymbol{\theta})\right\} = c_N E\left\{\hat{d}(\boldsymbol{\theta})\right\} \cong c_N \hat{d}(\boldsymbol{\theta}_0) \tag{17}$$

and

$$\text{bias}\left(\hat{\delta}(\boldsymbol{\theta})\right) = E\left\{\hat{\delta}(\boldsymbol{\theta})\right\} - \delta \cong c_N \hat{d}\left(\boldsymbol{\theta}_0\right) - \delta, \qquad (18)$$

respectively. Note that $\hat{d}\left(\boldsymbol{\theta}_0\right)$ does not depend on α and ϕ, it is a function of N and δ.

For N being fixed, to reduce the bias of $\hat{\delta}$ in (18) on the whole interval $-0.5 \le \delta \le 0.5$, we propose to determine the c_N such that the total square error between $c_N \hat{d}\left(\boldsymbol{\theta}_0\right)$ and δ on the interval $-0.5 \le \delta \le 0.5$, i.e.,

$$\int_{-0.5}^{0.5} \left(c_N \hat{d}\left(\boldsymbol{\theta}_0\right) - \delta\right)^2 d\delta \qquad (19)$$

is minimum. Taking the derivative of (19) with respect to c_N and equating the result to zero, we obtain

$$c_N = \int_{-0.5}^{0.5} \delta \hat{d}\left(\boldsymbol{\theta}_0\right) d\delta \Big/ \int_{-0.5}^{0.5} \left[\hat{d}\left(\boldsymbol{\theta}_0\right)\right]^2 d\delta. \qquad (20)$$

The following is a MATLAB programme for generating the bias correction factor c_N using (20).

```
function c_N=bias_correction_factor(w)
%w is the window function.
w=w(:)';
N=length(w);
n=[0:N-1]';
delta=0:0.01:0.5-0.01;
g=@(a) w*exp(1.0i*2*pi*n*a/N);
gd=g(delta);
gdm1=g(delta-1);
gdp1=g(delta+1);
deltahat=real((gdp1-gdm1)./...
   (2*gd-gdp1-gdm1));
c_N=sum(delta.*deltahat)/...
   sum(deltahat.^2);
```

Figure 1 shows biases of $\hat{\delta}$ given by (18) as a function of δ at $N = 16$ for the Hamming, Hann, Blackman, and Gauss windows without and with c_N.

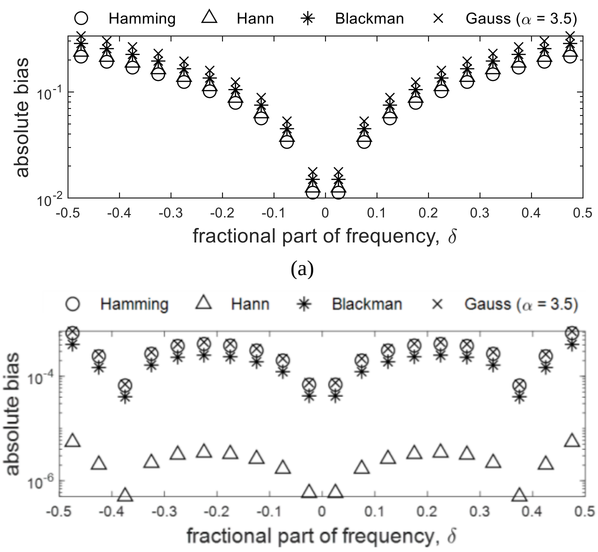

(a)

(b)

Fig. 1. Theoretical biases versus δ at $N = 16$ for different windows: (a) without c_N, and (b) with c_N.

It is observed that the percentage of reduction in the biases achieved by the inclusion of c_N was between 99.38 % and 99.99 % for the cases considered.

Note that (20) can be used to calculate a bias correction factor for any estimator $\hat{\delta}(\boldsymbol{\theta})$ for which $\hat{\delta}\left(\boldsymbol{\theta}_0\right)$ is a function only of N and δ.

B. Relation to Previous Results

– Bias Correction Factor

Under a small δ assumption, the expressions for c_N have been derived in [2] for the rectangle window, and in [5] for general windows. It can be shown that these expressions coincide with (20), when the function $\hat{d}\left(\boldsymbol{\theta}_0\right)$ in (20) is replaced by the first term of its Taylor series expansion around $\delta = 0$.

– Variance

Comparing (14) and the variance expressions derived under the small δ assumption in [4] and [5], it can be shown that they are identical only when $\delta = 0$ provided that

$$\sum_{n=0}^{N-1} w_n \sin\left(2\pi n/N\right) = 0. \qquad (21)$$

Figure 2 shows normalised variances, i.e., $\text{var}\left(\hat{\delta}\right) \times N \times \text{SNR}$, given by (14), ([4], (11)), and ([5], (13)) as a function of δ at $N = 16$ for the rectangle, Hamming, and Gauss windows (the condition (21) is satisfied by the rectangle and Hamming windows, while (21) does not hold for the Gauss window). We observe that the expressions in [4] and [5] agree with (14) only when, say, $|\delta| \le 0.1$, assuming that (21) is satisfied.

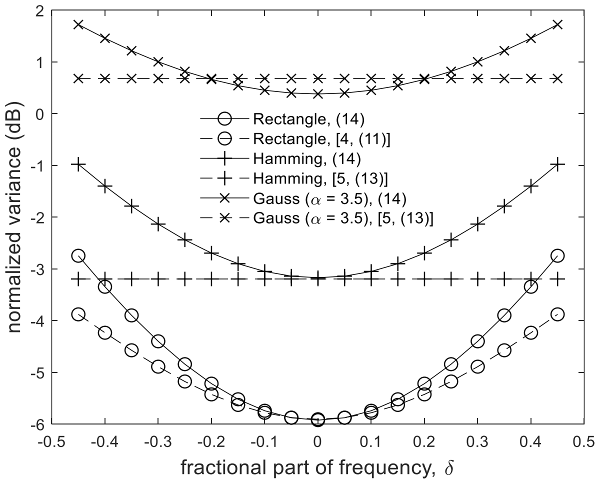

Fig. 2. Normalised theoretical variances versus δ at $N = 16$ for different windows.

III. THE CASE OF COSINE-SUM WINDOWS

The general variance expression in (14) will be examined for the case of cosine-sum windows. The cosine-sine window family is defined as

$$w_n = \sum_{p=0}^{P} (-1)^p a_p \cos\left(\frac{2\pi}{N} pn\right), n = 0,1,\ldots, N-1, \qquad (22)$$

subject to constraint $\sum_{p=0}^{P} a_p = 1.$ The rectangle, Hamming, Hann, Blackman and Blackman-Harris windows (see, e.g., [3]) are examples of windows from this family.

The window-dependent terms $g(\delta + l)$ and q_k in (6) and (12), respectively, are calculated for this family of windows as (see Appendix C)

$$g(\delta+l) = \frac{1}{2}\alpha e^{j\phi}\exp\left(j\pi\frac{N-1}{N}\delta\right)\sin(\pi\delta)\times \times\sum_{p=0}^{P}(-1)^p a_p\left[\exp\left(-j\frac{\pi}{N}(l+p)\right)\Big/\sin\left(\frac{\pi}{N}(\delta+l+p)\right)+ +\exp\left(-j\frac{\pi}{N}(l-p)\right)\Big/\sin\left(\frac{\pi}{N}(\delta+l-p)\right)\right],\ l=0,1,-1 \quad (23)$$

and

$$q_k = \frac{N}{4}\sum_{p,r=0}^{P}(-1)^{p+r}a_p a_r\left(\Delta_{p-r-k,sN}+\Delta_{p-r+k,sN}+ +\Delta_{p+r-k,sN}+\Delta_{p+r+k,sN}\right),\ k=0,1,2 \quad (24)$$

for $k = 0,1,2,$ where $\Delta_{p,r} =$ the Kronecker delta $(=1$ if $p = r,$ and $=0$ otherwise) and s is an integer.

From (23), $g(\delta+l) = O(N),$ implying that $\hat{d}(\boldsymbol{\theta}_0) = O(1),$ and thus c_N is $O(1)$ as $N \to \infty.$ Therefore, the limit of c_N as $N \to \infty,$ denoted by $c_\infty,$ may be used as an approximation to c_N for sufficiently large $N.$ Figure 3 shows c_N versus N for different cosine-sum windows. The limit c_∞ for each window is also shown. We see that c_N 's are well approximated by their limits for $N \geq 8.$

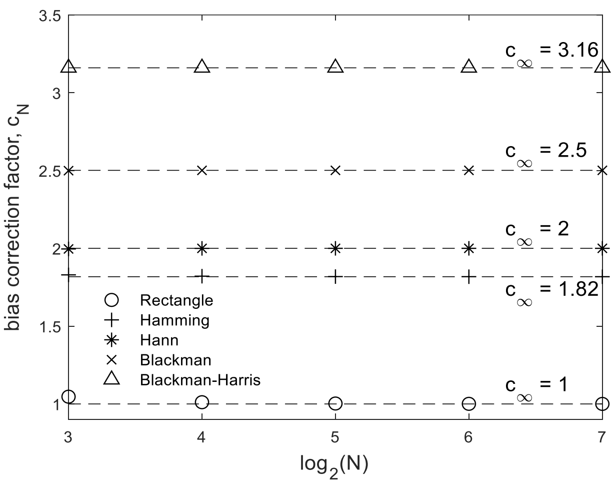

Fig. 3. Bias correction factor c_N versus N for different windows from the cosine-sum family. The dashed lines indicate the limit c_∞ of c_N as $N \to \infty$ for each window.

Note that the q_k 's are all real-valued for cosine-sum windows, so the variance expression in (14) simplifies as

$$\operatorname{var}(\hat{\delta}) \cong \frac{c_N^2 \lambda_N(\delta)}{N\,\mathrm{SNR}} \quad (25)$$

with

$$\lambda_N(\delta) = \frac{q_0}{2}\|\check{\mathbf{v}}\|^2 + q_1(\check{v}_1\check{v}_3 + \check{v}_2\check{v}_4 + \check{v}_3\check{v}_5 + \check{v}_4\check{v}_6) + q_2(\check{v}_1\check{v}_5 + \check{v}_2\check{v}_6). \quad (26)$$

A MATLAB programme to compute the $\lambda_N(\delta)$ in (25) for generic cosine-sum windows with coefficient vector $\{a_p\}_{p=0}^{P}$ is provided in Appendix D. Note that $\lambda_N(\delta)$ is the normalised variance, $\operatorname{var}(\hat{\delta}) \times N \times \mathrm{SNR},$ for $c_N = 1.$

Since $g(\delta+l) = O(N)$ and, from (24), q_k 's are also $O(N),$ it can be seen that $\lambda_N(\delta)$ in (26) is $O(1),$ as $N \to \infty.$ Replacing this term with its limit as $N \to \infty,$ denoted by $\lambda_\infty(\delta),$ together with the substitution of c_∞ for c_N in (25), an approximate expression of $\operatorname{var}(\hat{\delta})$ for sufficiently large N is obtained as

$$\operatorname{var}(\hat{\delta}) \cong \frac{c_\infty^2 \lambda_\infty(\delta)}{N\,\mathrm{SNR}}, \quad (27)$$

which gives the normalised variance as a function of δ only.

Figure 4 shows normalised variances given by (25) versus N for different values of δ for the Hamming window. The approximate variances given by (27) are also shown. We observe that (27) is a good approximation to (25) when $N \geq 8$ and for all δ considered. A weak dependence of the normalised variances on N is also noted; for each $\delta,$ the normalised variance is practically a constant function of N for $N \geq 8.$

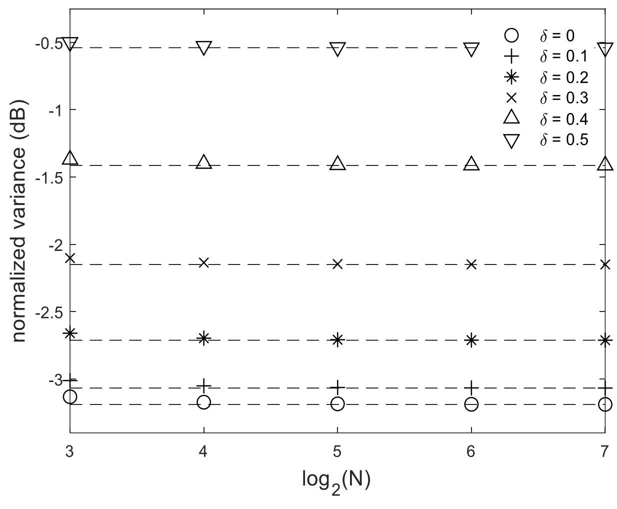

Fig. 4. Normalised theoretical variances versus N for different values of δ for the Hamming window. The variances given by (25) are shown with the markers, while the approximate variances by (27) are indicated by the dashed line.

IV. NUMERICAL EXAMPLES

Computer simulations were performed to validate our theoretical variance expressions for estimating the frequency of a complex sinusoid in complex white Gaussian noise. The sinusoid phase was set to zero. The amplitude of the sinusoid was set to 1 while different SNRs were obtained by properly scaling the noise samples. The frequency was $f = k_0 + \delta.$ The integer part k_0 of the frequency was treated as a known parameter and set to one fourth of the data length $N.$ The bias correction factor c_N was computed from (20). In each experiment, the Hamming, Hann, Blackman and Blackman-Harris windows from the cosine-sum family were applied to the data, respectively. The normalised variance of $\hat{\delta}$, $\operatorname{var}\left(\hat{\delta}\right) \times N \times \mathrm{SNR}$, was evaluated for each window as a function of δ and SNR. All simulation results were obtained by averaging 100000 independent runs.

Figure 5 shows normalised variances versus δ at $\mathrm{SNR} = 20$ dB, $N = 16$, and $k_0 = 4$. The expressions of (25) and (27) and the corresponding Cramér-Rao lower bound (CRLB), which is given by $\operatorname{var}\left(\hat{\delta}\right) \geq \dfrac{6N}{(2\pi)^2\, SNR\left(N^2 - 1\right)}$ (see, e.g. [8]), are also shown. We observe that the measured variances conformed well with the theoretical calculations of (25) while (27) was a good approximation for the whole range of δ. We also see that the estimator variance does not attain the CRLB. Figure 6 shows the results of the above experiment with $N = 128$ and $k_0 = 32$. Same observations were obtained; moreover, comparing normalised variances in Fig. 5 and Fig. 6, we see that increasing N by a factor of eight only very slightly changed the results, indicating the weak dependence of the normalised variances on N.

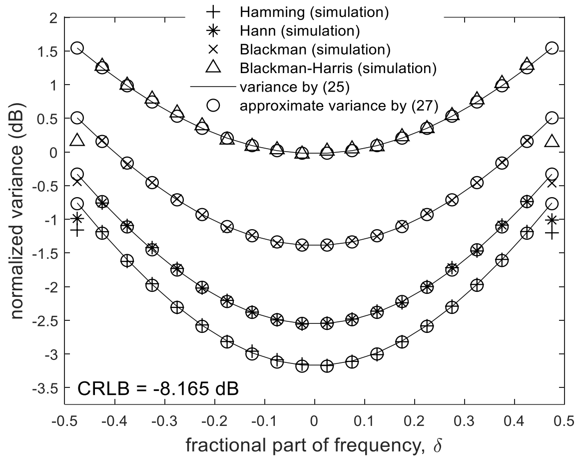

Fig. 5. Normalised variances versus δ at $\mathrm{SNR} = 20$ dB, $N = 16$, and $k_0 = 4$ for different cosine-sum windows.

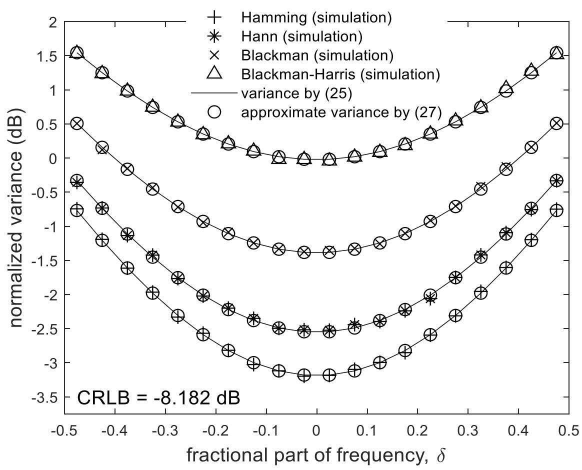

Fig. 6. As in Fig. 5, but for $N = 128$ and $k_0 = 32$.

Figure 7 shows normalised variances as a function of SNR at $\delta = 0.35$, $N = 128$, and $k_0 = 32$. It can be observed that (25) and (27) agreed well with the simulation results for $\mathrm{SNR} \geq 3$ dB.

The mean square error (MSE) is often used as a measure of the goodness of an estimator because it includes both the bias and variance of the estimator; it is given by $\mathrm{MSE} = \left(\mathrm{bias}\right)^2 + \left(variance\right)$.

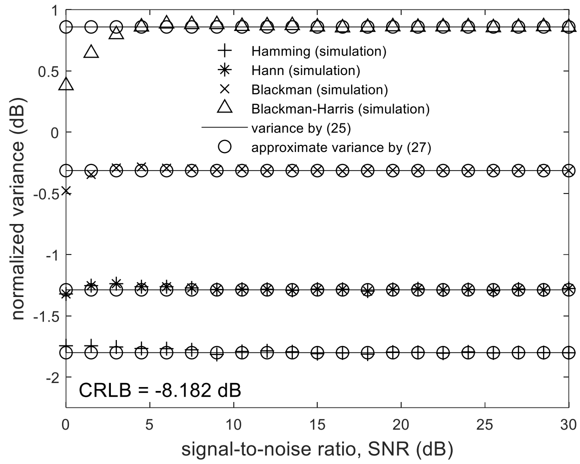

Fig. 7. Normalised variances versus SNR at $\delta = 0.35$, $N = 128$, and $k_0 = 32$ for different cosine-sum windows.

Figure 8 shows normalised variances together with mean square errors versus δ at $\mathrm{SNR} = 20$ dB, $N = 128$, and $k_0 = 32$. We see that measured mean square errors and variances are closely matched for the whole range of δ, indicating that the estimator is practically unbiased and that the mean square errors are well determined by the variances.

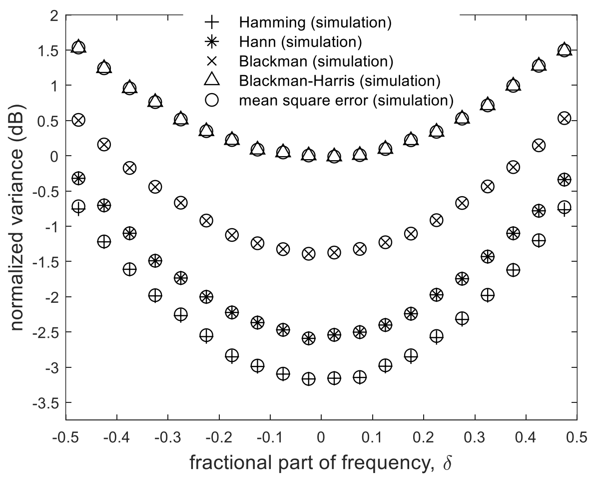

Fig. 8. Normalised variances and mean square errors versus δ at $\mathrm{SNR} = 20$ dB, $N = 128$, and $k_0 = 32$ for different cosine-sum windows.

Figure 9 shows normalised variances and mean square errors as a function of SNR at $\delta = 0.35$, $N = 128$, and $k_0 = 32$. We note the close agreement between mean square errors and variances for all SNR's.

V. CONCLUSIONS

An exact general frequency variance expression of the frequency estimators suggested by Jacobsen [1] and Candan [2] has been derived for a single complex sinusoid in complex white noise for the case of windowed data.

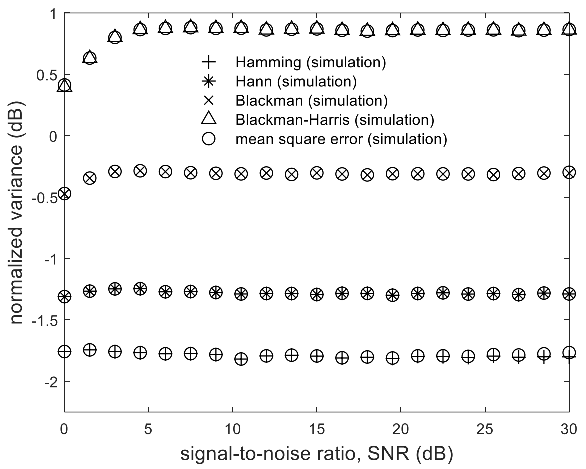

Fig. 9. Normalised variances and mean square errors versus SNR at $\delta = 0.35$, $N = 128$, and $k_0 = 32$ for different cosine-sum windows.

A general formula for the bias correction factor c_N has been presented. A MATLAB implementation of c_N was also provided. The variance expression was examined for the case of cosine-sum windows and a MATLAB programme that calculates the normalised variance for this case was given. With a number of cosine-sum windows, both c_N and the normalised variance were shown to have a weak dependence on N. An approximate variance formula for sufficiently large N was also developed for the cosine-sum window family. All the theoretical results have been verified by computer simulations under different conditions.

APPENDIX A

– *Derivation of* $\boldsymbol{\theta}_0$

Noise samples satisfy the following conditions:

$$E\{e_n\} = 0, \tag{A.1}$$

$$E\{e_n e_m^*\} = \begin{cases} \sigma^2, & \text{if } n = m, \\ 0, & \text{if } n \neq m, \end{cases} \tag{A.2}$$

$$E\{e_n e_m\} = 0, \ \text{for all } n, m, \tag{A.3}$$

where E denotes the expectation operator and superscript * denotes the complex conjugate.

Let $W_N = \exp\left(j\frac{2\pi}{N}\right)$. Then

$$\begin{bmatrix} E\{X_{k_0-1}\} = E\left\{\sum_{n=0}^{N-1} w_n x_n W_N^{-(k_0-1)n}\right\} = \\ = E\left\{\sum_{n=0}^{N-1}\left(\alpha e^{j\phi} w_n W_N^{(k_0+\delta)n} + w_n e_n\right) W_N^{-(k_0-1)n}\right\} = \\ = \alpha e^{j\phi}\sum_{n=0}^{N-1} w_n W_N^{(\delta+1)n} + \\ + \sum_{n=0}^{N-1} w_n E\{e_n\} W_N^{-(k_0-1)n} = \\ = \alpha e^{j\phi}\sum_{n=0}^{N-1} w_n W_N^{(\delta+1)n} = g(\delta+1) \end{bmatrix} \tag{A.4}$$

using (A.1). Similarly, $E\{X_{k_0}\} = g(\delta)$ and $E\{X_{k_0+1}\} = g(\delta-1)$.

– *Derivation of* $\mathbf{C_0}$

The elements of $\mathbf{C_0}$ are either $\operatorname{cov}(\bar{X}_k, \bar{X}_l)$, or $\operatorname{cov}(\tilde{X}_k, \tilde{X}_l)$, or $\operatorname{cov}(\bar{X}_k, \tilde{X}_l)$ for $k, l = k_0 - 1$, k_0, and $k_0 + 1$, where $\operatorname{cov}(X, Y) = E\{(X - E\{X\})(Y - E\{Y\})\}$, i.e., the covariance between the real random variables X and Y. We have, using (A.1)–(A.3)

$$\begin{bmatrix} E\left\{(X_k - E\{X_k\})(X_l - E\{X_l\})^*\right\} \\ = E\left\{\left(\sum_{n=0}^{N-1} w_n e_n W_N^{-kn}\right)\left(\sum_{m=0}^{N-1} w_m e_m^* W_N^{lm}\right)\right\} = \\ = \sum_{n,m=0}^{N-1} w_n w_m E\{e_n e_m^*\} W_N^{-kn+lm} = \\ = \sigma^2 \sum_{n=0}^{N-1} w_n^2 W_N^{-(k-l)n} = \begin{cases} \sigma^2 q_{k-l}, & \text{for } k \geq l, \\ \sigma^2 q_{|k-l|}^*, & \text{for } k < l. \end{cases} \end{bmatrix} \tag{A.5}$$

and

$$\begin{bmatrix} E\left\{(X_k - E\{X_k\})(X_l - E\{X_l\})\right\} = \\ = E\left\{\left(\sum_{n=0}^{N-1} w_n e_n W_N^{-kn}\right)\left(\sum_{m=0}^{N-1} w_m e_m W_N^{-lm}\right)\right\} = \\ = \sum_{n,m=0}^{N-1} w_n w_m E\{e_n e_m\} W_N^{-kn-lm} = \\ = 0, \ \text{for all } k, l \end{bmatrix}. \tag{A.6}$$

On the other hand,

$$E\left\{(X_k - E\{X_k\})(X_l - E\{X_l\})^*\right\} = \\ = \left[\operatorname{cov}(\bar{X}_k, \bar{X}_l) + \operatorname{cov}(\tilde{X}_k, \tilde{X}_l)\right] + j\left[\operatorname{cov}(\tilde{X}_k, \bar{X}_l) - \operatorname{cov}(\bar{X}_k, \tilde{X}_l)\right] \tag{A.7}$$

and

$$E\left\{(X_k - E\{X_k\})(X_l - E\{X_l\})\right\} = \\ = \left[\operatorname{cov}(\bar{X}_k, \bar{X}_l) - \operatorname{cov}(\tilde{X}_k, \tilde{X}_l)\right] + j\left[\operatorname{cov}(\tilde{X}_k, \bar{X}_l) + \operatorname{cov}(\bar{X}_k, \tilde{X}_l)\right]. \tag{A.8}$$

From (A.5)–(A.8), it follows that

$$\operatorname{cov}(\bar{X}_k, \bar{X}_l) = \operatorname{cov}(\tilde{X}_k, \tilde{X}_l) = \frac{\sigma^2}{2}\bar{q}_{|k-l|} \tag{A.9}$$

and

$$\operatorname{cov}(\tilde{X}_k, \bar{X}_l) = \operatorname{sgn}(k-l)\frac{\sigma^2}{2}\tilde{q}_{|k-l|}. \tag{A.10}$$

The expression of $\mathbf{C_0}$ in (10) now follows from (A.9) and (A.10).

APPENDIX B

Proof of phase independence of variance. Decompose $g(\delta + l)$ as

$$g(\delta + l) = e^{j\phi} h(\delta + l), \tag{B.1}$$

where

$$h(\delta + l) = \alpha \sum_{n=0}^{N-1} w_n \exp\left(j\frac{2\pi}{N}(\delta + l)n\right) \tag{B.2}$$

for $l = 0,1,-1.$ From (B.1), we have

$$\bar{g}(\delta+l)=\bar{h}(\delta+l)\cdot\cos\phi-\tilde{h}(\delta+l)\cdot\sin\phi \tag{B.3}$$

and

$$\tilde{g}(\delta+l)=\bar{h}(\delta+l)\cdot\sin\phi+\tilde{h}(\delta+l)\cdot\cos\phi. \tag{B.4}$$

Putting (B.3) and (B.4) into (5), we can express $\boldsymbol{\theta}_0$ as

$$\boldsymbol{\theta}_0=\mathbf{M}(\phi)\boldsymbol{\omega}_0, \tag{B.5}$$

where

$$\mathbf{M}(\phi)=\begin{bmatrix}\cos\phi & -\sin\phi & & & & \\ \sin\phi & \cos\phi & & & & \\ & & \cos\phi & -\sin\phi & & \\ & & \sin\phi & \cos\phi & & \\ & & & & \cos\phi & -\sin\phi \\ & & & & \sin\phi & \cos\phi\end{bmatrix} \tag{B.6}$$

and

$$\boldsymbol{\omega}_0=\left[\bar{h}(\delta+1),\tilde{h}(\delta+1),\bar{h}(\delta),\tilde{h}(\delta),\bar{h}(\delta-1),\tilde{h}(\delta-1)\right]^{\mathrm{T}}. \tag{B.7}$$

Let variables $\boldsymbol{\theta}$ and $\boldsymbol{\omega}$ be related as $\boldsymbol{\theta}=\mathbf{M}(\phi)\boldsymbol{\omega}.$ Then we have, using the chain rule and the fact that $\hat{d}(\mathbf{M}(\phi)\boldsymbol{\omega})=\hat{d}(\boldsymbol{\omega})$

$$\mathbf{v}=\nabla\hat{d}(\boldsymbol{\theta})\Big|_{\boldsymbol{\theta}=\boldsymbol{\theta}_0=\mathbf{M}(\phi)\boldsymbol{\omega}_0}=\mathbf{M}(\phi)\nabla\hat{d}(\boldsymbol{\omega})\Big|_{\boldsymbol{\omega}=\boldsymbol{\omega}_0}=\mathbf{M}(\phi)\mathbf{u}, \tag{B.8}$$

where $\mathbf{u}=\nabla\hat{d}(\boldsymbol{\omega})\Big|_{\boldsymbol{\omega}=\boldsymbol{\omega}_0}$, which does not depend on ϕ.

It follows from (B.8) that

$$\|\mathbf{v}\|^2=\|\mathbf{u}\|^2 \tag{B.9}$$

since the matrix $\mathbf{M}(\phi)$ is orthogonal. Also,

$$\begin{aligned} &v_1v_3+v_2v_4+v_3v_5+v_4v_6= \\ &=(u_1\cos\phi-u_2\sin\phi)(u_3\cos\phi-u_4\sin\phi)+ \\ &+(u_1\sin\phi+u_2\cos\phi)(u_3\sin\phi+u_4\cos\phi)+ \\ &+(u_3\cos\phi-u_4\sin\phi)(u_5\cos\phi-u_6\sin\phi)+ \\ &+(u_3\sin\phi+u_4\cos\phi)(u_5\sin\phi+u_6\cos\phi)= \\ &=u_1u_3+u_2u_4+u_3u_5+u_4u_6 \end{aligned} \tag{B.10}$$

and, similarly,

$$v_1v_4-v_2v_3+v_3v_6-v_4v_5=u_1u_4-u_2u_3+u_3u_6-u_4u_5, \tag{B.11}$$

$$v_1v_5+v_2v_6=u_1u_5+u_2u_6, \tag{B.12}$$

$$v_1v_6-v_2v_5=u_1u_6-u_2u_5. \tag{B.13}$$

Substituting the results in (B.9)−(B.13) from (13) shows that (13) is independent of ϕ.

APPENDIX C

– Proof of (23)

We have

$$\begin{aligned} g(\delta+l)&=\alpha e^{j\phi}\sum_{n=0}^{N-1}w_n\exp\left(j\frac{2\pi}{N}(\delta+l)n\right)= \\ &=\alpha e^{j\phi}\sum_{n=0}^{N-1}\sum_{p=0}^{P}(-1)^p a_p\cos\left(\frac{2\pi}{N}pn\right)\exp\left(j\frac{2\pi}{N}(\delta+l)n\right)= \\ &=\tfrac{1}{2}\alpha e^{j\phi}\sum_{p=0}^{P}(-1)^p a_p\times \\ &\times\sum_{n=0}^{N-1}\left[\exp\left(j\frac{2\pi}{N}(\delta+l+p)n\right)+\exp\left(j\frac{2\pi}{N}(\delta+l-p)n\right)\right]. \end{aligned} \tag{C.1}$$

The result in (23) now follows, since

$$\begin{aligned} &\sum_{n=0}^{N-1}\exp\left(j\tfrac{2\pi}{N}(\delta+l+p)n\right)= \\ &=\exp\left(j\pi\tfrac{N-1}{N}\delta\right)\sin(\pi\delta)\left[\exp\left(-j\tfrac{\pi}{N}(l+p)\right)\Big/\sin\left(\tfrac{\pi}{N}(\delta+l+p)\right)\right] \end{aligned} \tag{C.2}$$

for integers $l, p.$

– Proof of (24)

We have

$$\begin{aligned} w_n^2&=\sum_{p,r=0}^{P}(-1)^{p+r}a_pa_r\cos\left(\frac{2\pi}{N}pn\right)\cos\left(\frac{2\pi}{N}rn\right)= \\ &=\frac{1}{2}\sum_{p,r=0}^{P}(-1)^{p+r}a_pa_r\left[\cos\left(\frac{2\pi}{N}(p-r)n\right)+\cos\left(\frac{2\pi}{N}(p+r)n\right)\right]= \\ &=\frac{1}{4}\sum_{p,r=0}^{P}(-1)^{p+r}a_pa_r\times \\ &\times\left[\exp\left(j\frac{2\pi}{N}(p-r)n\right)+\exp\left(-j\frac{2\pi}{N}(p-r)n\right)+\right. \\ &\left.+\exp\left(j\frac{2\pi}{N}(p+r)n\right)+\exp\left(-j\frac{2\pi}{N}(p+r)n\right)\right]. \end{aligned} \tag{C.3}$$

Thus,

$$\begin{aligned} q_k&=\sum_{n=0}^{N-1}w_n^2\exp\left(-j\frac{2\pi}{N}kn\right)= \\ &=\frac{1}{4}\sum_{p,r=0}^{P}(-1)^{p+r}a_pa_r\times \\ &\times\sum_{n=0}^{N-1}\left[\exp\left(j\frac{2\pi}{N}(p-r-k)n\right)+\exp\left(-j\frac{2\pi}{N}(p-r+k)n\right)+\right. \\ &\left.+\exp\left(j\frac{2\pi}{N}(p+r-k)n\right)+\exp\left(-j\frac{2\pi}{N}(p+r+k)n\right)\right]. \end{aligned} \tag{C.4}$$

The result in (24) now follows because

$$\sum_{n=0}^{N-1}\exp\left(\pm j\frac{2\pi}{N}pn\right)=N\Delta_{p,sN} \tag{C.5}$$

for integers $p, s.$

APPENDIX D

Computation of normalised variance for cosine-sum windows

```
function lambda=norm_var(a,N,delta)
%INPUTS:
% a       window’s coefficient vector
% N       window’s length
% delta   fractional part of frequency
%
%OUTPUT:
% lambda  normalised variance with bias
```

```
%         correction factor equal to one
q=[];
for k=0:2
qk=0;sp=1;
for p=1:length(a)
sr=sp;
for r=1:length(a)
qk=qk+sr*a(p)*a(r)*...
  (~(mod(p-r-k,N))+~(mod(p-r+k,N))+...
  ~(mod(p+r-2-k,N))+~(mod(p+r-2+k,N)));
sr=-sr;
end
sp=-sp;
end
q=[q qk];
end
q=0.25*q;
gd=0;gdp1=0;gdm1=0;s=1;
for p=1:length(a)
gd=gd+s*a(p)*...
  (exp(-1.0i*pi*(p-1)/N)/...
  sin(pi*delta/N+pi*(p-1)/N)+...
  exp(1.0i*pi*(p-1)/N)/...
  sin(pi*delta/N-pi*(p-1)/N));
gdp1=gdp1+s*a(p)*...
  (exp(-1.0i*pi*p/N)/...
  sin(pi*delta/N+pi*p/N)+...
  exp(1.0i*pi*(p-2)/N)/...
  sin(pi*delta/N-pi*(p-2)/N));
gdm1=gdm1+s*a(p)*...
  (exp(-1.0i*pi*(p-2)/N)/...
  sin(pi*delta/N+pi*(p-2)/N)+...
  exp(1.0i*pi*p/N)/...
  sin(pi*delta/N-pi*p/N));
s=-s;
end
m=0.5*exp(1.0i*pi*(N-1)*delta/N)*...
  sin(pi*delta);
gd=gd*m;gdp1=gdp1*m;gdm1=gdm1*m;
v=grad_vec([real(gdp1),imag(gdp1),...
  real(gd),imag(gd),...
  real(gdm1),imag(gdm1)]);
lambda=N^2*(0.5*q(1)*norm(v)^2+...
  q(2)*(v(1)*v(3)+v(2)*v(4)+...
  v(3)*v(5)+v(4)*v(6))+...
  q(3)*(v(1)*v(5)+v(2)*v(6)));
%---------------------------------------%
function vcup0=grad_vec(theta0)
theta=sym('theta',[1 6]);
t1=theta(1)+1.0i*theta(2);
t2=theta(3)+1.0i*theta(4);
t3=theta(5)+1.0i*theta(6);
dhat=real((t1-t3)/(2*t2-t1-t3));
vcup=gradient(dhat);
vcup0=double(subs(vcup,theta,theta0));
```

CONFLICTS OF INTEREST

The authors declare that they have no conflicts of interest.

REFERENCES

[1] E. Jacobsen and P. Kootsookos, “Fast, accurate frequency estimators”, *IEEE Signal Processing Magazine*, vol. 24, no. 3, pp. 123−125, 2007. DOI: 10.1109/MSP.2007.361611.

[2] Ç. Candan, “A method for fine resolution frequency estimation from three DFT samples”, *IEEE Signal Processing Letters*, vol. 18, no. 6, pp. 351−354, 2011. DOI: 10.1109/LSP.2011.2136378.

[3] F. J. Harris, “On the use of windows for harmonic analysis with the discrete Fourier transform”, *Proceedings of the IEEE*, vol. 66, no. 1, pp. 51−83, 1978. DOI: 10.1109/PROC.1978.10837.

[4] Ç. Candan, “Analysis and further improvement of fine resolution frequency estimation method from three DFT samples”, *IEEE Signal Processing Letters*, vol. 20, no. 9, pp. 913−916, 2013. DOI: 10.1109/LSP.2013.2273616.

[5] Ç. Candan, “Fine resolution frequency estimation from three DFT samples: Case of windowed data”, *Signal Processing*, vol. 114, pp. 245−250, 2015. DOI: 10.1016/j.sigpro.2015.03.009.

[6] B. M. Keyta and E. Dilaveroğlu, “An exact analysis of fine resolution frequency estimation method from three DFT samples”, *Uludağ University Journal of the Faculty of Engineering*, vol. 30, no. 1, 2025. DOI: 10.17482/uumfd.1583908.

[7] A. Papoulis, *Probability, Random Variables, and Stochastic Processes*, 3rd ed. New York: McGraw-Hill, 1991.

[8] S. M. Kay, *Fundamentals of Statistical Signal Processing: Estimation Theory*. New Jersey: Prentice-Hall, 1993.